This paper is available on line at http://www.mcponline.org

Phosphoproteome Dynamics Upon Changes in Plant Water Status Reveal Early Events Associated With Rapid Growth Adjustment in Maize Leaves*[S]

Ludovic Bonhomme‡‖, Benoît Valot§, François Tardieu¶, and Michel Zivy‡‖

Plant growth adjustment during water deficit is a crucial adaptive response. The rapid fine-tuned control achieved at the post-translational level is believed to be of considerable importance for regulating early changes in plant growth reprogramming. Aiming at a better understanding of early responses to contrasting plant water statuses, we carried out a survey of the protein phosphorylation events in the growing zone of maize leaves upon a range of water regimes. In this study, the impact of mild and severe water deficits were evaluated in comparison with constant optimal watering and with recovery periods lasting 5, 10, 20, 30, 45, and 60 min. Using four biological replicates per treatment and a robust quantitative phosphoproteomic methodology based on stable-isotope labeling, we identified 3664 unique phosphorylation sites on 2496 proteins. The abundance of nearly 1250 phosphorylated peptides was reproducibly quantified and profiled with high confidence among treatments. A total of 138 phosphopeptides displayed highly significant changes according to water regimes and enabled to identify specific patterns of response to changing plant water statuses. Further quantification of protein amounts emphasized that most phosphorylation changes did not reflect protein abundance variation. During water deficit and recovery, extensive changes in phosphorylation status occurred in critical regulators directly or indirectly involved in plant growth and development. These included proteins influencing epigenetic control, gene expression, cell cycle-dependent processes and phytohormone-mediated responses. Some of the changes depended on stress intensity whereas others depended on rehydration duration, including rapid recoveries that occurred as early as 5 or 10 mins after rewatering. By combining a physiological approach and a quantitative phosphoproteomic analysis, this work provides new insights into the *in vivo* early phosphorylation events triggered by rapid changes in plant water status, and their possible involvement in plant growth-related processes. ***Molecular & Cellular Proteomics 11: 10.1074/mcp.M111.015867, 957–972, 2012.***

The maintenance of crop productivity upon reduced water resources will be a challenging issue to ensure food production under future climate conditions. Water deficit induces a wide range of responses at the whole plant, cellular and molecular levels (1). Among adjustments triggered by water deficit, leaf growth is one of the earliest and most sensitive processes that occurs independently of photosynthetic rates and plant carbon status (2, 3), which tends to show that growth reduction is a crucial adaptive response (4). A reduced leaf growth limits water losses by transpiration *via* a decreased leaf area but also limits the potential light interception. This reduces biomass accumulation and further, leads to substantial yield losses. Thus, leaf growth reduction has both a positive effect on plant stress avoidance and a negative effect on final crop yields. The optimization balance between the control of water losses and the potential carbon assimilation can differ according to climatic scenarios and increasing knowledge on its determinism may allow future progress in the maintenance of crop production on changing plant water statuses. In maize, leaf growth is restricted to the base of the leaf in a 6 to 8 cm-long fragment, named the growing zone (5, 6). This growing zone includes tissues in which both cell division and cell expansion happen, partly overlapping in time and space (6). Cells are produced near the leaf base in the meristematic region, pushing forward the expanding cells into the distal regions of the leaf growing zone. Upon water deficit, leaf growth reprogramming is achieved by modulating both cell division and cell expansion (7–9). Previous analyses have already reported that altered plant growth occurs concomitantly with changes in cyclin-dependent kinase activity, in cell wall expansion genes (such as expansin genes), in turgor or in cell wall properties (5, 10–14). In a recent paper, pioneer efforts in identifying the earliest molecular events controlling cell division upon osmotic stress have evidenced that ethylene signaling acts upstream on the cell cycle arrest

From the ‡INRA/University Paris-Sud/CNRS/AgroParisTech, UMR 0320/UMR 8120 Génétique Végétale, Gif-sur-Yvette, 91190, France; §INRA, Plateforme d'Analyse Protéomique de Paris Sud Ouest, PAPPSO, Gif-sur-Yvette, 91190, France; ¶INRA, Laboratoire d'Ecophysiologiedes Plantes sous Stress Environnementaux, LEPSE, Montpellier, 34060, France

Received November 15, 2011, and in revised form, June 14, 2012
Published, MCP Papers in Press, July 10, 2012, DOI 10.1074/mcp.M111.015867

and on cyclin-dependent kinase A activity, independently to a transcriptional control (15). However, the molecular mechanisms involved in the rapid plant growth adjustment in water stress responses is still fragmentary.

Phosphorylation of proteins is of considerable importance for regulating plant growth (16). As a rapid and transient post-translational modification, protein phosphorylation achieves a fine-tuned regulation of protein function in a wide array of cellular processes during development or in response to environmental cues, from signaling cascades to gene expression (17). Therefore, early protein phosphorylation and dephosphorylation events could play a pivotal role in the rapid growth adjustment occurring in plants facing water limitation. Studying phosphoproteome dynamics has already proven to be a useful strategy to decipher sucrose-induced responses in cell cultures (18) or ABA[1]-dependent changes *in planta* (19) for instance, but early responses to changing plant water status at the level of a growing tissue have not yet been well documented. To our knowledge, data dealing with water deficit-induced changes in protein phosphorylation have been mainly obtained from long-term stressed plants (20, 21), and no time-course analysis of rapid *in vivo* changes has been explored.

To investigate relations between early phosphorylation events and growth, the present exploratory study was carried out *in planta* on the phosphoproteome of the leaf growing zone of maize plants submitted to contrasting water statuses. Quantitative changes in phosphorylation status were assessed in two scenarios of water stress, an early and mild water deficit as well as a more severe one (MWD and SWD, respectively). Because water deficit is usually fluctuating in the fields with dehydration and rewatering events, we also analyzed a sequence of rehydration that causes rapid recovery of leaf elongation rate in maize. In maize, the full recovery of leaf growth occurs 40 min after rehydration, which is even faster than the recovery of leaf water potential (22). In addition, rewatering is instantaneous and enables to accurately define the response time to the changes in plant water status.

EXPERIMENTAL PROCEDURES

Plant Growth and Monitoring of Dehydration and Rehydration Conditions—Seeds of the maize (*Zea mays* L.) inbred line B73 were grown in 1-L pots filled with a soil:compost (2:3, v/v) mixture. Plants were grown in a growth cabinet at a light intensity of 450 μmol/m^2/s (16 h photoperiod, 25 °C day and 18 °C night), with 50% air relative humidity. The design involved four randomized complete blocks (one biological replicate of each treatment per block), each surrounded with two bordering rows of supplementary plants. During the first hour of light, pots were weighed and watered to maintain a soil humidity of 60% (optimal irrigation) and the length of the fifth leaf was measured from pot edge to tip. Experimental treatment began when the fifth leaf reached a length of 30 cm (day 0), about 3 weeks after sowing. Control plants were maintained at a constant soil water status and two water deficits were imposed to other plants by withholding water, namely mild (MWD) and severe water deficit (SWD). MWD plants were sampled on day 1 whereas SWD plants were collected when the growth of the sixth leaf reached less than 1 cm/d, on days 4–5. A batch of SWD plants were rewatered to soil retention capacity and sampled 5, 10, 20, 30, 45, and 60 min after rewatering (RH_5, RH_{10}, RH_{20}, RH_{30}, RH_{45}, and RH_{60}, respectively). Control plants of the same ontogenic stage as stressed plants, were sampled on day 1 ($CTRL_1$) and on days 4–5 when the fourth leaf ceased to grow ($CTRL_2$). Five-centimeter-long fragments (cm 1 to 6 from leaf insertion point) of the leaf growing zone were harvested between the sixth and the seventh hour of light. Four biological replicates were collected for each treatment. Samples were immediately frozen in liquid nitrogen and stored at −80 °C. For each biological replicate, midday leaf water potential (Ψ_{md}, MPa) was measured with a Scholander-type pressure chamber (PMS-670; PMS Instrument) on the fourth leaf (the last ligulated leaf) at the time of sampling.

Protein Extraction and In-solution Digestion—Leaf fragments were finely ground in a ball crusher (TissuLyser, Qiagen) cooled with liquid nitrogen. For each collected sample, a denaturing protein extraction using a trichloroacetic acid/acetone procedure was achieved as described in Méchin *et al.* (23), except that 40 μl of resolubilization solution [6 M urea, 2 M thiourea, 2% 3-[(3-cholamidopropyl)dimethylammonio]propanesulfonate (m/v), 30 mM Tris-HCl pH 7,8] was used to resuspend 1 mg of pellet. Protein content was determined using the 2-D Quant-kit (GE Healthcare), with bovine serum albumin (BSA) as standard. For each biological replicate, 1.5 mg of proteins were collected and reduced with DTT at a final concentration of 10 mM. Samples were subsequently alkylated with iodoacetamide at a final concentration of 40 mM. Both steps were performed during 45 min. The samples were diluted to $<$ 2 M urea by adding 50 mM ammonium bicarbonate. Protein digestion (Trypsin Gold; Promega, Madison, WI) was performed at an enzyme/substrate ratio of 1:20 (w:w) by overnight incubation at 37 °C, and stopped by adding 1% formic acid (v/v).

Stable Isotope Dimethyl Labeling by Reductive Amination of Tryptic Peptides—Tryptic peptides were dried *in vacuo* and resuspended in 1 ml of 5% formic acid (v/v). Stable isotope dimethyl labeling was performed according to the on-column procedure described by Boersema *et al.* (24) using formaldehyde-H2 (light labeling) or formaldehyde-D_2 (heavy labeling). Each sample was loaded on a separate SepPak C18 cartridge column (3 ml; Waters) and washed with 0.6% acetic acid (v/v). SepPak columns were flushed ten times with 1 ml of the respective labeling reagent (50 mM sodium phosphate buffer pH 7.5, 30 mM NaBHCN and 0.2% CH_2O or CD_2O (v/v) for light or heavy labeling, respectively). Labeled samples were eluted with 500 μl of 0.6% acetic acid (v/v) and 80% acetonitrile (ACN) (v/v). Biological replicates were labeled with the light isotope whereas an internal standard was labeled with the heavy isotope. The internal standard was designed by pooling equivalent amounts of peptides from each treatment. All heavy dimethyl-labeled peptides were homogenized before being mixed with the light dimethyl-labeled peptides in a 1:1 abundance ratio.

Peptide Fractionation Using Strong Cation Exchange Chromatography (SCX)—Prior to SCX, the dimethyl-labeled peptides were dried by vacuum centrifugation and subsequently reconstituted in 500 μl of solvent A (30% ACN (v/v), 5% formic acid (v/v), pH 2.5). SCX was performed at 200 μl/min using Zorbax BioSCX-Series II columns (0.8-mm inner diameter × 50-mm length; 3.5 μm particle size) and a Famos autosampler (LC Packings). After sample loading, the first 17 min were run isocratically at 100% solvent A, followed by an increas-

[1] The abbreviations used are: ABA, abscisic acid; MWD, mild water deficit; SWD, severe water deficit; RH_5, RH_{10}, RH_{20}, RH_{30}, RH_{45}, and RH_{60}, rewatering duration of 5, 10, 20, 30, 45 and 60 min, respectively; SCX, strong cation exchange chromatography; FDR, false discovery rate; XIC, extracted ion chromatogram; SOTA, self organizing tree algorithm; CL, SOTA cluster.

ing pH gradient using solvent B (30% ACN (v/v), 5% formic acid (v/v), 540 mM ammonium formate, pH 4.7). SCX fractions were automatically collected using an on-line Probot system (LC Packings).

Selective Enrichment of Phosphopeptides Using Immobilized Metal Ion Affinity Chromatography (IMAC)—SCX fractions were dried and resuspended in 300 μl of solvent C (250 mM acetic acid, 30% ACN (v/v)). Peptides were gently mixed with 80 μl of Phos-Select iron affinity gel (Sigma-Aldrich) and incubated for 1.5 h using a tube rotator, as described by Nühse *et al.* (25). The mixture was transferred into SigmaPrep spin columns (Sigma-Aldrich) and the flow-through fractions containing the nonphosphorylated peptides were collected. Iron affinity gel with bound phosphopeptides was rinsed twice with 200 μl of solvent C, then once with 200 μl of double distilled water. The elution of bound phosphopeptides was achieved with 100 μl of solvent D (400 mM NH_4OH, 30% ACN) by centrifugation at 8200 g. Flow-through fractions and eluted phosphopeptides were dried and kept at −20 °C until LC-MS/MS analysis.

LC-MS/MS Analysis—On-line liquid chromatography was performed on a NanoLC-Ultra system (Eksigent). A 4 μl sample was loaded at 7.5 μl/min on a precolumn cartridge (stationary phase: C18 PepMap 100, particles of 5 μm; column: 100 μm i.d., 1 cm length; Dionex) and desalted with 0.1% formic acid in water. After 3 min, the precolumn cartridge was connected to the separating PepMap C18 column (stationary phase: C18 PepMap 100, particles of 3 μm; column: 75 μm i.d., 150 mm length; Dionex). Buffers were 0.1% formic acid in water (E) and 0.1% formic acid in ACN (F). Peptide separation was achieved using a linear gradient from 5 to 30% F at 300 nl/min.

Eluted peptides were analyzed with a LTQ XL ion trap (Thermo Electron) using a nano-electrospray interface. Ionization (1.5 kV ionization potential) was performed with liquid junction and a noncoated capillary probe (10 μm i.d.; New Objective). For phosphopeptide analysis, peptide ions were analyzed using Xcalibur 2.07 with the following data-dependent acquisition steps: (1) a full MS scan was recorded in enhanced scan rate mode for higher resolution and mass accuracy (mass-to-charge ratio (*m/z*) 300 to 1400, profile mode), (2) an MS/MS spectrum was acquired on the two highest-intensity species detected in the preceding MS scan (qz = 0.25, activation time = 30 ms, and collision energy = 35%; profile mode), and (3) an MS^3 scan was triggered when a neutral loss of 98 or 80 Da was detected in the preceding MS/MS scan. Dynamic exclusion was set to 30 s. Non-phosphopeptides were analyzed using Xcalibur 2.07 with the following data-dependent acquisition steps: (1) a full MS scan (mass-to-charge ratio (*m/z*) 300 to 1400, profile mode) and (2) MS/MS (qz = 0.25, activation time = 30 ms, and collision energy = 35%; profile mode). Steps 2 was repeated for the three major ions detected in step 1. Dynamic exclusion was set to 30 s.

Identification of Peptides and Phosphorylation Sites—Database searches were performed using X!Tandem (http://www.thegpm.org/TANDEM/; 2010.01.01.4). Enzymatic cleavage was described to be because of trypsin digestion with one possible miscleavage. Cys carboxyamidomethylation and, light and heavy dimethylation of peptide N termini and lysine residues were set as static modifications whereas Met oxidation and phosphorylation of tyrosine, serine and threonine residues were set as variable modifications. Precursor mass and fragment mass tolerance were 2.0 and 0.5 Da, respectively. Identifications were performed using the MaizeSequence genome database (Release 4a.53, 53764 entries, October 2009, http://maizesequence.org) supplemented by the maize UniProt database (Release 15.11, 43694 entries, December 2009, http://www.uniprot.org) and by a contaminant database (trypsin, keratins, *etc*). Identified proteins were filtered and grouped using the X! Tandem pipeline v3.1.2, a bioinformatic tool developed by the PAPPSO platform (http://pappso.inra.fr/bioinfo/xtandempipeline/). Data filtering was achieved according to a peptide E value smaller than 0.01. The false discovery rate (FDR) at the peptide level was assessed from searches against a decoy database (using the reversed amino acid sequence for each protein). All peptide sequences and phosphorylation sites showing a significant water regime effect were confirmed by manual inspection of the raw data to verify the peptide sequence and the phosphorylation site assignment.

Identified MaizeSequence sequences and UniProt maize sequences matching unknown proteins were searched against the UniProtKB Plant database using the BLAST tool (http://www.uniprot.org/). Proteins were classified into functional groups according to the UniProtKB database, the DBGET system (http://www.genome.ad.jp/dbget/) or based on information retrieved from already published works.

Quantification of Peptides and Phosphorylation Sites—Relative quantification of nonphosphorylated peptides and phosphopeptides was performed using the MassChroQ software (26) by extracting ion chromatograms (XICs) of all identified peptides within a 0.3 Th window and by integrating the area of the XIC peak at their corresponding retention time. LC-MS/MS data alignment was performed using the "MS/MS method" that uses common MS/MS identifications as landmarks to evaluate retention time deviations along the chromatographic profile. Alignments were performed within groups of LC-MS/MS runs originating from similar SCX fractions. The following parameters were used: ms2 tendency halfwindow = 10 and ms2 smoothing halfwindow = 15. For each peptide detected in the heavy and light form in a single LC-MS/MS run, a light to heavy ratio was computed. To compensate for possible global variations between LC-MS/MS runs, a normalization step was performed by dividing ratios by their median value in each LC-MS/MS run. Only nonphosphopeptides were used for quantitation of protein amounts. Subsequent statistical analyses were performed on $\log_2$-transformed normalized data.

Data Availability—Raw MS output files, identified phosphopeptides and their corresponding spectra were uploaded to the ProticDB database (27). The data can be directly visualized or downloaded from http://moulon.inra.fr/protic/phospho. Tandem mass spectral data are also available via the Proteomics Identifications database (PRIDE) at http://www.ebi.ac.uk/pride/under the accession numbers 24901 to 26498. A detailed list of all peptides identified in all LC-MS/MS runs is given in supplemental Table S1, representative spectra of each phosphopeptide displaying significant water regime effect are shown in supplemental Fig. S1, and relative quantification data are available in supplemental Table S2.

Statistical Analysis—Results were analyzed with the R programming language v2.11.1 (R Development Core Team, 2010). Significance of water regime-dependent changes in phosphopeptide abundance was tested using a one-way ANOVA with the following model: $Y_{ik} = \mu + T_i + \varepsilon_{ik}$; in which Y_{ik} refers to individual values, μ is the general mean, T_i is the effect of treatment i ($i = 10$) and ε_{ik} is the residual ($k = 4$). The R package QVALUE (version 1.1) was used to calculate q-values from the resulting p values assessed from the ANOVA. A q-value (28) lower than 0.05 was defined in order to control the positive false-discovery rate at a 5% level. Using such requirements, a p value < 0.01 was considered to be significant. A Self Organizing Tree Algorithm (SOTA) clustering was performed on phosphopeptides showing significant changes using the Multi Experiment Viewer (MEV) software (http://www.tm4.org/mev/). Clustering was performed from Z score transformed values, with the Pearson correlation as dissimilarity criteria, 10 cycles and a p value of 0.05 for determining the variability division criteria. The significance of recovery was assessed from the linear regression of phosphopeptide abundance on the duration of rehydration, including SWD to RH_{60}. The relationship between protein phosphorylation changes and midday leaf water potential was evaluated by rank correlations (Kendall's tau

coefficient, τ) performed by computing the average values observed in $CTRL_2$ and in each time point of the rehydration kinetics, ranging from SWD to RH_{60}. Changes in protein abundance were evaluated in response to SWD and RH_{60}, in comparison to $CTRL_2$ and SWD, respectively. Both effects were tested using a one-way ANOVA with a model similar as above.

RESULTS

Plant Growth and Physiological Response to Changes in Plant Water Status—In our experimental design, plants were submitted to a range of water regimes including a mild and a severe water deficit (MWD and SWD), and rehydration periods lasting 5, 10, 20, 30, 45, and 60 min starting from SWD (RH_5, RH_{10}, RH_{20}, RH_{30}, RH_{45}, and RH_{60}, respectively). Each water regime led to homogeneous phenotypes. Under optimal irrigation, the evapotranspiration increased along with plant growth, whereas it declined relative to control plants, by 35% during MWD and by about 70% during SWD (Fig. 1*A*). Compared with control conditions, water deficit led to a 12% and a 22% decrease of soil water content in MWD and SWD, respectively (Fig. 1*A* inset). The growth decrease of the 5th leaf was initiated during MWD and a 90% growth drop was observed as a result of SWD (Fig. 1*B*). Although MWD induced changes in evapotranspiration, in soil water status and in plant growth, it was not sufficient to affect midday leaf water potential (Ψ_{md}, Fig. 1*C*), which suggested that plants controlled water losses *via* stomatal regulation (29). On the opposite, SWD resulted in an extensive decrease in Ψ_{md} by nearly 1 MPa. Rehydration events induced a significant partial recovery of Ψ_{md} as early as 20 min after rewatering (Fig. 1*C*), emphasizing that water transport had recovered in plants at that time.

Assessing the Dynamics of Protein Phosphorylation Status in the Growing Zone of Maize Leaves—To assess a comprehensive scheme of the protein phosphorylation dynamics in the growing zone of maize leaves, we designed a quantitative phosphoproteomic approach based on stable isotope incorporation at the peptide level using dimethyl labeling. Stable isotope dimethyl labeling has already proven to be a useful strategy for assessing reciprocal measurements between treatments (30) in a single MS analysis using the mass difference of the dimethyl labels. In this study, an alternative labeling strategy was designed: the same internal standard was systematically mixed with all analyzed samples at a 1:1 ratio. The internal standard was designed by pooling an equivalent amount of peptides from all the analyzed samples (Fig. 2). To control for any isotope effect, the internal standard peptide mixture was labeled with the same heavy isotope composition whereas all analyzed samples were labeled with the light isotope composition (Fig. 2). Thus, samples from all treatments were analyzed exactly the same way, and the use of the internal standard maximized the number of peptides for which quantification was possible on both the heavy and the light isotope labels. After mixing the internal standard with each biological replicate, peptide mixtures were submitted to

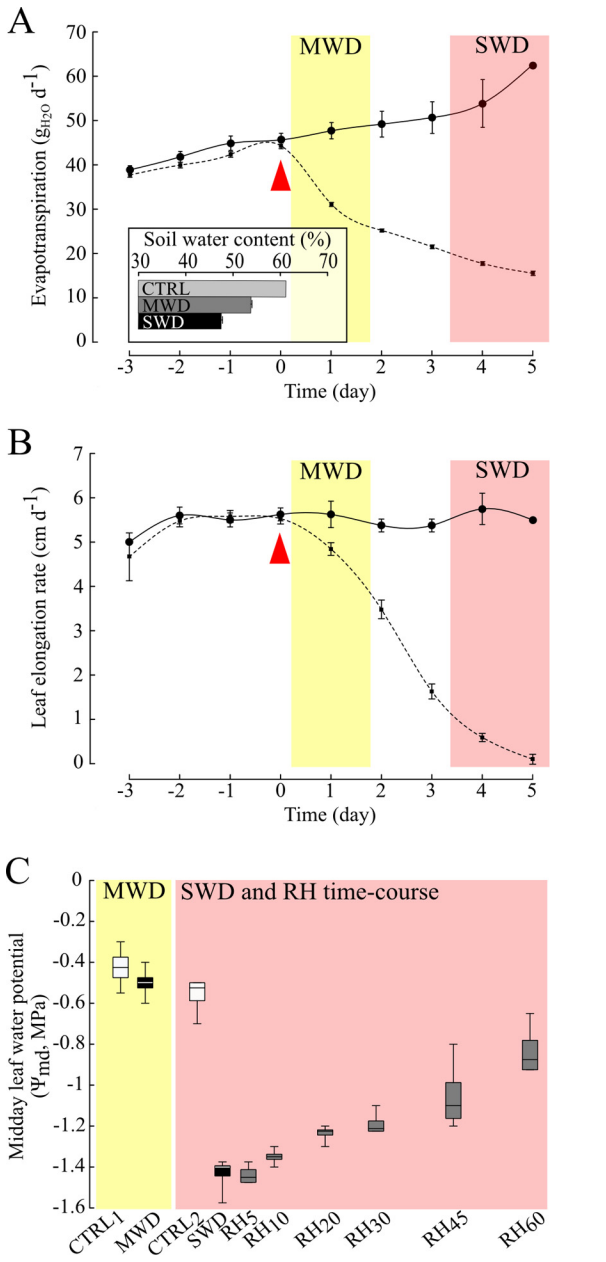

FIG. 1. **Evapotranspiration, leaf growth, and plant water status characterization.** *A*, the evapotranspiration (g_{H2O}/d) is shown for control (*black line*, $n = 8$) and stressed (*broken line*, $n = 32$) plants. Mean values ± S.E. are shown. The *red arrow* indicates the beginning of water shortage in stressed plants. The inset shows the soil water content assessed in control (CTRL, $n = 8$), mild water deficit (MWD, $n = 4$), and severe water deficit (SWD, $n = 28$) treatments. *B*, the elongation rate of the fifth leaf (cm/d) is depicted for control (*black line*, $n = 8$) and stressed (*broken line*, $n = 32$) plants. Mean values ± S.E. are shown. *C*, the midday leaf water potential of plants (Ψ_{md}, MPa) was measured concomitantly to the samplings of the leaf growing zone. Each box represents the quartile below (Q1) and above (Q3) the median value. Vertical bars show minimum and maximum values. Box plots are shown for mild water deficit (MWD), severe water deficit (SWD), and for the rehydration time course (RH_5 to RH_{60}), in comparison to control plants ($CTRL_1$ and $CTRL_2$) at the same ontogenic development.

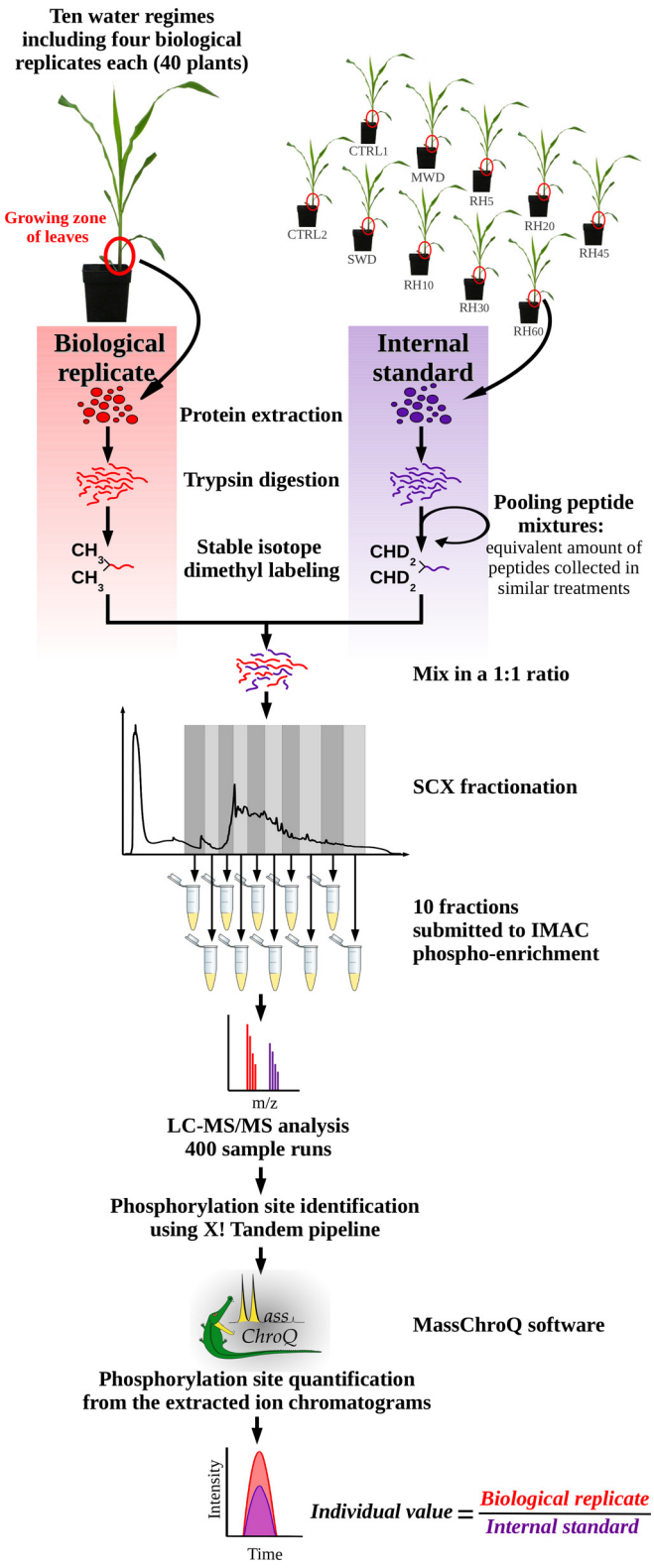

FIG. 2. **Experimental work flow used for analyzing the phosphoproteome of the growing zone of maize leaves.** Each biological replicate was individually analyzed relative to an internal standard. The internal standard was designed by pooling equivalent amounts of digested peptides from all analyzed plants. Peptide samples were then submitted to prefractionation prior to phosphopeptide enrichment. Phosphorylated peptides were analyzed using LC-MS/MS and relative quantification was achieved by XIC extraction.

an SCX prefractionation, yielding ten individual eluates (Fig. 2). Each eluate was submitted to affinity chromatography over IMAC-(Fe^{3+}) for phosphopeptide enrichment. As a whole, 400 LC-MS/MS runs were carried out (ten per sample), which resulted in the identification of 80,217 phosphopeptides at a false discovery rate of $< 0.5\%$ (supplemental Table S1). They accounted for 3,664 unique phosphorylation sites (Fig. 3*A*) belonging to 2,496 different phosphoproteins. Phosphopeptide abundances were then compared through their extracted ion chromatograms (XIC). Here, 3604 nonredundant phosphorylation sites were quantified, accounting for 297,034 individual quantitative values. Considering all the quantified phosphorylation sites, nearly 60% were observed in both light and heavy isotope forms within each LC-MS/MS run (Fig. 3*B*). According to our strategy, phosphorylation site quantification was achieved by computing their light to heavy ratio in each LC-MS/MS run, which required that both isotope envelopes had been extracted from the total ion current. Before any normalization, the median value of the raw ratios was nearly 1 (supplemental Fig. S2). After normalization, quantitative changes of phosphopeptides were assessed from ratios that were quantified in at least 2/3 of all biological replicates (Fig. 3*A*). This stringent criterion offered a high confidence for approving the phosphorylation site identification and relative quantification. Furthermore, most of the reported phosphorylation sites were identified from MS/MS spectra recorded in more than one biological replicate and in more than one experimental condition (supplemental Table S1).

Impact of Contrasting Plant Water Statuses on Protein Phosphorylation in the Growing Zone of Maize Leaves—Among 1235 reproducible phosphopeptides (Fig. 3*A*), 132 displayed highly significant quantitative changes ($p < 0.01$) in response to water regimes and 6 showed unambiguous qualitative changes (Table I, supplemental Table S3). Qualitative changes concerned three phosphorylation sites that were not detected upon MWD only, another one that was not detected upon SWD only, and two others that were reproducibly detected only during SWD and the rehydration time-course. Overall, quantitative and qualitative changes concerned 124 unique proteins mainly involved in chromatin remodeling (18%), in cell division or cell expansion-related processes (16%), in phytohormone-responses or signaling (14%), in transcription regulation (7%), and in carbohydrate metabolism (6%) (Fig. 4*A*). Other processes were related to protein metabolism (4%), energy metabolism (4%), stress response (3%), and other miscellaneous processes (9%). Proteins whose function could not be ascertained ("unknown proteins") accounted for 19% of the significant changes.

To uncover patterns in the changes in protein phosphorylation during dehydration and rehydration, a self organizing

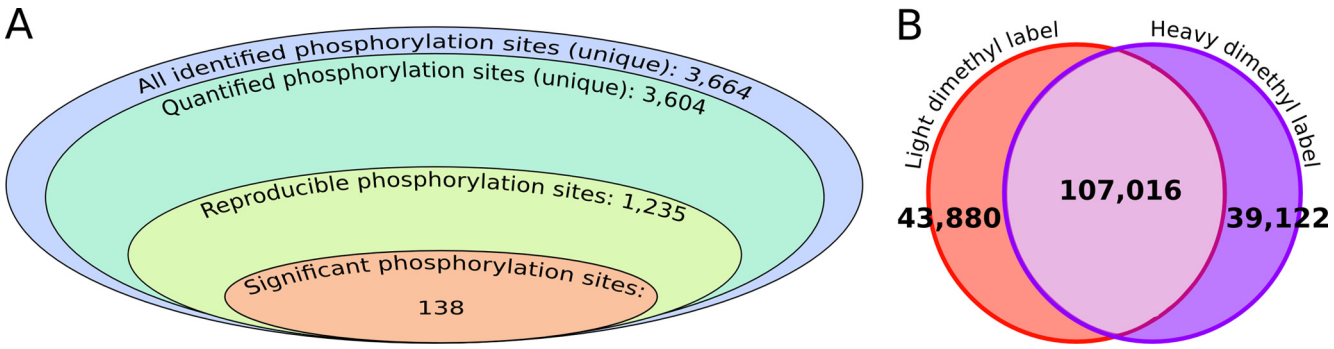

FIG. 3. **Results of large-scale phosphorylation site identification and quantification.** *A*, overview of the number of phosphorylation sites throughout the work flow of the quantitative analysis. *B*, Venn diagram depicting the number of quantifications of all phosphorylated peptides in light- and heavy-dimethyl labeled forms.

tree algorithm (SOTA) was used on phosphorylated peptides showing significant abundance variations (Fig. 5 and supplemental Fig. S3). Seven main clusters with distinct phosphorylation dynamics, gathered more than 91% of the whole quantitative kinetic profiles (Fig. 5). Regardless of the whole cluster patterns, the largest variations of phosphorylation status were observed in response to SWD, either through decreasing or increasing abundances. Among SWD-induced changes, more than the half were not detected during MWD or were not exceeding ± 25% of the SWD variation, and about 16% displayed opposite changes (Fig. 6*A*). However, part of the SWD-induced changes was already observed upon MWD and most of them varied with a smaller magnitude, as evidenced in CL5 for instance (Fig. 5). The abundance of 30 phosphorylated peptides displayed a variation in response to MWD ranging from 25% to 75% of that detected during SWD, whereas comparable changes (75% to 125% of that detected during SWD) accounted for four phosphorylation sites (Fig. 6*A*). Changes in abundance of higher magnitude during MWD compared with SWD, referred to five phosphorylated peptides. Furthermore, although CL1 or CL4 reflected persistent SWD-induced changes even after a 60 min-long rewatering, CL3, CL6, and CL7 depict that part of the SWD-induced changes partially or fully recovered along with the rehydration time-course (Fig. 5). These three clusters included 60% of the observed changes belonging to phytohormone-related and signaling proteins, 45% of those evidenced on transcription regulators, one third of those related to chromatin-related or cell cycle-related proteins, and less than 12% of those involved in the other identified processes (Fig. 4*B*). In addition, CL2, CL6, and CL7 clusters showed that part of the changes displayed sudden and reversible variations within the rehydration time course. These transitory changes were mainly observed for protein kinases or phosphatases in the range of 10 to 30 min after rewatering. As a whole, nearly 40% of the 132 phosphopeptides showing a significant quantitative change, displayed at least a half-recovery to their control level at one of the time points of the rehydration kinetic. To assess the occurrence of a recovery, a linear regression was computed from phosphopeptide abundances *versus* duration of the rewatering events. Although the expected response was not necessarily linear, this enables to detect protein phosphorylation statuses which recovered at least partially to the status of the control plants. A significant linear regression ($p < 0.05$) was detected for 36 phosphopeptides (Fig. 6*B*) among which ten showed a highly significant Kendall correlation ($p < 0.02$) of their abundance along with the Ψ_{md} changes (Table I, supplemental Table S3 and supplemental Fig. S4). In all significant linear regressions except one, the change in abundance over the rehydration time-course was consistent with a recovery. Interestingly, more than a half-recovery was observed for three and six phosphorylation sites as early as 5 and 10 min rewatering respectively, whereas 23 were observed after 60 min rehydration, including 14 that displayed more than a 90% recovery (Fig. 6*B*).

Furthermore, the abundance of proteins displaying water regime-responsive phosphopeptides was explored. To quantify protein abundance, we investigated their nonphosphorylated peptides (NP) found in the IMAC flow-through fractions (FT). Since SCX prefractionation intrinsically delays NP elution (data not shown), only the seven last FT per biological replicate (among the 10 available ones) were analyzed. NP was traced in SWD plants in comparison to $CTRL_2$, and in RH_{60} relative to SWD *i.e.* a total of 84 LC-MS/MS runs. Among the 124 unique proteins showing phosphopeptide quantitative variations, 83 were identified with at least one specific NP. Reproducible quantitative values were reliably obtained for 49 proteins (Table I and supplemental Table S3). This result emphasizes that phosphopeptide enrichment obviously enabled the identification of very low-abundance phosphorylated proteins. This substantially prevents joint quantification of both NP and phosphopeptides for many proteins because of contrasting dynamic range. Relative to $CTRL_2$, SWD induced significant changes in NP abundances for only six proteins, including five covariations between NP and phosphopeptide abundance changes (Table I, supplemental Table S3 and Supplemental Fig. S5). Only one protein, a

TABLE I

Partial list of phosphorylation sites significantly affected by changing plant water statuses

			Phosphopeptides								Non phosphopeptides	
Accession	Description	UniProtKB Id[a]	Phosphosite[b]	*P*-value[c]	MWD / CTRL$_1$[d]	SWD / CTRL$_2$[e]	MWD / SWD[f]	RH recovery > 50%[g]	τ[h]	SOTA[i]	SWD / CTRL$_2$[j]	RH$_{60}$ / SWD[k]
Carbohydrate metabolism												
tr|B8A307|B8A307_MAIZE	Citrate transporter family protein	B6U1B5	S241	1.4E-03	1.37	1.58	> 50%			CL5		
GRMZM2G055331_P01	Sucrose phosphate synthase A	E1APE3	S168	6.1E-04	0.87	1.34				CL4	ns	ns
GRMZM2G055331_P08	Sucrose phosphate synthase A	E1APE3	S95	7.3E-03	1.29	1.03	> 50%			CL5	ns	ns
GRMZM2G060659_P02	Sucrose synthase 3	Q8L5H0	T846	1.6E-03	1.06	1.44				CL5	2.89	0.35
GRMZM2G039588_P02	Galactose mutarotase-like	A2Q396	S158	7.0E-04	1.16	1.35		*		CL8		
GRMZM2G023289_P03	Phosphoglucomutase, cytoplasmic 2	P93805	S106	4.5E-03	0.86	1.20				CL4	ns	ns
tr|B6U8S7|B6U8S7_MAIZE	Carbohydrate transporter/ sugar porter/ transporter	B6U8S7	S5	1.5E-03	1.02	0.37				CL2		
GRMZM2G004932_P01	6-phosphofructokinase	B6SVM3	S79	2.7E-09	1.08	4.97		*	-0.8	CL7	ns	ns
Cell division or cell expansion-related proteins												
GRMZM2G071249_P01	Proline-rich cell wall protein-like	B6TN35	S49	5.1E-03	0.67	0.44		RH$_{60}$*	0.7	CL3	ns	ns
tr|B8A0C4|B8A0C4_MAIZE	Villin-3, putative, expressed	Q10L72	S900/T902	7.6E-08	1.30	1.63	> 50%			CL5	ns	ns
tr|C0PCF2|C0PCF2_MAIZE	Golgi SNARE 12 protein	B6TXF5	S56	2.4E-07	0.90	0.43		RH$_{10, 30, 45, 60}$*	0.8	CL3		
GRMZM2G012031_P01	AIR9 protein	Q00NU6	S59	3.9E-06	0.89	1.54				CL6		
GRMZM2G027723_P01	Cellulose synthase-2	Q9LLI8	S158/S165	2.4E-04	1.08	0.42				CL2		
GRMZM2G015875_P02	Nuclear matrix constituent protein 1	D2YZU5	S934	7.8E-04	1.17	1.51				CL5		
GRMZM2G097900_P01	Calmodulin-related protein 2, touch-induced	B6TV01	S66	1.3E-03	0.90	1.56				CL4	ns	ns
GRMZM2G320689_P04	Kinesin heavy chain	Q93XG0	T952	9.4E-07	1.02	0.26				CL2		
tr|B6SKE1|B6SKE1_MAIZE	Sterol 3-beta-glucosyltransferase	B6SKE1	S74/T75	5.0E-04	1.01	1.61				CL4		
GRMZM2G128206_P02	Pollen-specific protein SF3	B6SU00	S79	4.5E-03	1.06	0.52				CL1	ns	ns
GRMZM2G052078_P02	CLIP-associating protein 1-like	Q6KAI5	T1161	3.1E-03	0.70	0.97	> 50%	RH$_{5, 10, 20, 30, 45, 60}$*		CL10	ns	ns
tr|B6TBM4|B6TBM4_MAIZE	USP family protein	B6TBM4	S35	1.9E-04	0.91	0.83	> 50%	RH$_{5, 10, 20, 30, 45, 60}$*	0.7	CL3	ns	ns
tr|B4FCK0|B4FCK0_MAIZE	USP family protein	B6TBM4	S30	6.6E-05	1.06	0.92		RH$_{10, 20, 30, 45, 60}$*		CL8	ns	ns
GRMZM2G406674_P02	Calmodulin binding protein	B6T984	S345	1.3E-04	1.67	1.41	> 50%			CL5	ns	ns
GRMZM2G465169_P01	Microtubule-associated protein MAP65-1a	B6U4I4	S557	7.5E-04	0.86	0.60		RH$_{60}$*		CL3	ns	ns
tr|B4FT16|B4FT16_MAIZE	Vacuolar protein sorting 26	B6UEZ8	S221	7.5E-08	0.95	1.70				CL4	ns	ns
tr|B8A180|B8A180_MAIZE	GTP-ase activating protein for Arf containing protein	B6U114	S312/S313	5.1E-05	0.99	1.92				CL4	ns	ns
GRMZM2G341732_P02	GTP-ase activating protein for Arf containing protein	B6U114	S340/S341/S343	6.3E-04	0.92	2.42				CL8		
tr|B8A180|B8A180_MAIZE	GTP-ase activating protein for Arf containing protein	B6U114	S241	4.6E-03	0.92	0.99	> 50%	RH$_{5, 10, 20, 30, 45, 60}$		CL9	ns	ns
GRMZM2G176612_P02	ADP-ribosylation factor GTPase-activating protein 3	B6TII3	S406	3.7E-04	0.83	2.38		RH$_{60}$		CL6	ns	ns
GRMZM2G092741_P01	Adaptin N terminal region family protein	Q10SS6	S65	p/a	p/a	1.04		RH$_5$		CL9		
GRMZM2G178398_P01	Putative epsin	Q948G6	S273	p/a	p/a	p/a				CL6	ns	ns
Chromatin remodeling												
GRMZM2G103345_P02	R3h domain containing protein, Putative	B9SG72	T278	3.0E-03	0.97	1.18				CL4		
GRMZM2G125648_P01	HMG1/2-like protein	B6T1S6	S159	1.9E-05	1.05	0.16				CL2		
tr|B6TWE3|B6TWE3_MAIZE	HMGI/Y protein	Q9FER8	S151	7.3E-04	1.04	0.73				CL1	ns	ns
tr|Q9FYS5|Q9FYS5_MAIZE	High mobility group I/Y-2	Q9FYS5	S155/S157	1.1E-05	1.04	0.67		*		CL1	ns	ns
tr|B4FZG8|B4FZG8_MAIZE	Putative uncharacterized protein (IPR005819 Histone H5)	B4FZG8	S395	3.0E-04	1.07	0.33				CL2	ns	ns
GRMZM2G121840_P01	HemK methyltransferase family member 2	B6TML1	S255	7.9E-03	0.91	0.58		RH$_{60}$*		CL3		
GRMZM2G025592_P01	DNA (cytosine-5)-methyltransferase 1	Q9AXT8	S118	7.1E-09	0.92	0.24				CL1		
GRMZM2G025592_P01	DNA (cytosine-5)-methyltransferase 1	Q9AXT8	S5	3.3E-08	0.76	0.12				CL1		
GRMZM2G157470_P01	Putative methyl-binding domain protein MBD115	Q5I204	S138/T144	6.6E-03	1.00	1.53		RH$_{45, 60}$*		CL7	ns	ns
GRMZM2G157470_P01	Putative methyl-binding domain protein MBD115	Q5I204	S341	3.7E-06	0.90	0.57				CL1	ns	ns
tr|B6TRL2|B6TRL2_MAIZE	Putative methyl-binding domain protein MBD105	Q94IQ9	S252	1.5E-05	1.40	1.38	> 50%			CL5	ns	ns
tr|B6TRL2|B6TRL2_MAIZE	Putative methyl-binding domain protein MBD105	Q94IQ9	S332	2.0E-03	1.31	1.54	> 50%	RH$_{60}$		CL5	ns	ns
tr|B6TRL2|B6TRL2_MAIZE	Putative methyl-binding domain protein MBD105	Q94IQ9	S300	9.0E-05	1.09	1.21				CL5	ns	ns
tr|B7ZZV6|B7ZZV6_MAIZE	Putative pumilio/Mpt5 family RNA-binding protein	Q94HK0	S210	3.5E-04	1.41	1.56	> 50%			CL5		
tr|B7ZZV6|B7ZZV6_MAIZE	Putative pumilio/Mpt5 family RNA-binding protein	Q94HK0	S249/S250	9.0E-06	0.97	1.40				CL4		
GRMZM2G012964_P01	Putative pumilio/Mpt5 family RNA-binding protein	Q94HK0	S245/S246/S247	9.0E-05	0.84	1.56				CL6	ns	ns
GRMZM2G012964_P01	Putative pumilio/Mpt5 family RNA-binding protein	Q94HK0	S202	8.0E-05	0.90	1.49		RH$_{45}$*		CL7	ns	ns
GRMZM2G012964_P01	Putative pumilio/Mpt5 family RNA-binding protein	Q94HK0	S31/T35	1.4E-04	1.21	1.77		RH$_{45}$*		CL7	ns	ns
GRMZM2G159032_P04	Histone deacetylase 2b	B6SK06	S101	4.3E-09	0.75	0.47				CL1	ns	ns
sp|Q9M4U5|HDT2_MAIZE	Histone deacetylase HDT2	Q9M4U5	S105	6.1E-03	0.93	0.87	> 50%			CL2	ns	ns
GRMZM2G443814_P02	Plus-3 domain containing protein, expressed	O7XCX5	S373	1.0E-03	1.79	0.49		RH$_{5, 10, 30, 60}$*		CL3		
GRMZM2G334722_P01	Putative uncharacterized protein (IPR001005 SANT, DNA-binding)	B6TY92	S56	9.6E-06	0.99	0.58		RH$_{60}$*		CL3		
GRMZM2G704338_P02	Bromo-adjacent homology (BAH) domain-containing protein-like	Q6Z809	S744	9.1E-03	1.08	1.42		RH$_{20, 45, 60}$*		CL7	ns	ns
GRMZM2G010075_P02	Bromodomain-containing protein, putative	B9SGL2	S124	2.4E-04	0.63	2.20		*		CL6		
GRMZM2G375984_P01	Protein DEK, putative	B9RAB2	S115	8.4E-03	1.48	0.53		RH$_{20, 45}$		CL2		
Phytohormone-related and signaling proteins												
GRMZM2G016939_P03	Protein kinase G11A	B6U4S9	S665	5.8E-03	0.36	2.93				CL10		
sp|B6TNQ7|U7376_MAIZE	Ninja-family protein 6	B6TNQ7	S83	2.0E-12	1.71	3.02				CL5		
GRMZM2G438290_P01	Ninja-family protein 5	B6SM63	S105	6.6E-04	1.08	3.80				CL4		

TABLE I—*continued*

			Phosphopeptides								Non phosphopeptides	
Accession	Description	UniProtKB Id[a]	Phosphosite[b]	*P*-value[c]	MWD / $CTRL_1$[d]	SWD / $CTRL_2$[e]	MWD / SWD[f]	RH recovery > 50%[g]	τ[h]	SOTA[i]	SWD / $CTRL_2$[j]	RH_{60} / SWD[k]
GRMZM2G334165_P03	Serine/threonine-protein kinase PBS1, putative	B9SP66	S157, S161	2.5E-03	0.73	1.04				CL10		
GRMZM2G413544_P01	Putative Ste-20 related kinase, 3'-partial	Q8W2Y7	S351	1.7E-03	0.77	1.62		RH_{20}		CL6		
tr|B6T6P6|B6T6P6_MAIZE	Serine/threonine-protein kinase SAPK10	B6T6P6	S173	2.1E-14	2.39	5.59	> 50%			CL5		
GRMZM2G702514_P01	Naringenin,2-oxoglutarate 3-dioxygenase	B6TMV8	S17	4.6E-03	1.91	1.33	> 50%	$RH_{10, 45, 60}$		CL11		
GRMZM2G125424_P01	MDR-like ABC transporter	Q8GU77	S382	4.1E-04	0.88	0.35				CL2		
GRMZM2G085236_P02	MDR-like ABC transporter	Q8GU76	S541	5.3E-04	0.95	0.30		RH_{60}*		CL3	ns	ns
GRMZM2G066274_P01	Receptor-like kinase RHG1	Q7FQF1	S753	7.7E-03	p/a	2.24		$RH_{20, 60}$*		CL6	ns	ns
tr|B6SQ98|B6SQ98_MAIZE	Protein phosphatase inhibitor 2 containing protein	B6SQN8	S5	9.9E-03	1.04	0.85		RH_{60}		CL3		
GRMZM2G110922_P04	SnRK2.4	D5FGN9	S158	4.8E-03	1.27	2.05		$RH_{10, 20}$		CL6		
tr|B4FI84|B4FI84_MAIZE	GCK-like kinase MIK	Q6Y2W8	S204	9.3E-04	1.07	0.51		$RH_{20, 30, 45, 60}$*		CL3	ns	ns
GRMZM2G451132_P01	Serine/threonine-protein kinase ctr1	Q7XXN2	T433	3.3E-03	0.83	3.20				CL6		
GRMZM2G011070_P01	Salt-inducible protein kinase	Q5XTZ4	S431	1.1E-03	1.02	1.62		$RH_{20, 60}$*		CL6		
GRMZM2G099049_P02	Auxin-repressed protein	B6TRA9	S29/S31	2.2E-03	1.09	3.13		RH_{60}		CL6	p/a	ns
GRMZM2G099049_P02	Auxin-repressed protein	B6TRA9	T118	1.1E-03	0.82	4.04				CL4	p/a	ns
tr|B4FO41|B4FO41_MAIZE	Auxin-repressed 12.5 kDa protein	B6TOX4	S59/S60/S61/T66	6.3E-08	1.01	4.26		*	-0.7	CL6		
tr|C4J107|C4J107_MAIZE	Map3k delta-1 protein kinase, putative	B9RZR2	T326	p/a	p/a	0.63		$RH_{30, 60}$		CL3		
tr|C0PIZ1|C0PIZ1_MAIZE	Serine/threonine-protein phosphatase	C5YZZ9	T169	p/a	0.89	p/a				CL7		
Transcription regulators												
tr|A5HEH4|A5HEH4_MAIZE	GIF2	A5HEH4	S212	9.5E-04	1.03	0.48				CL2		
GRMZM2G132636_P01	DNL zinc finger family protein	B6TGI7	T12, S21	6.7E-03	1.28	1.24	> 50%			CL5		
GRMZM2G077596_P01	COP1-interacting protein 7 (CIP7)-like protein	Q7XI09	S855	2.8E-03	0.91	1.20				CL8		
tr|B6UHC7|B6UHC7_MAIZE	Transcription factor HY5	B6UHC7	S43	2.7E-03	0.81	0.49				CL3		
GRMZM2G360517_P03	Protein TIME FOR COFFEE	Q94KE2	S1329	8.0E-04	0.94	0.64		$RH_{45, 60}$*		CL3		
GRMZM2G360517_P03	Protein TIME FOR COFFEE	Q94KE2	S1341	9.5E-05	1.00	0.74				CL2		
GRMZM2G403636_P01	DEAD-box ATP-dependent RNA helicase 52C	Q2R1M8	T71/S76	2.7E-03	0.76	1.43				CL8	ns	ns
tr|C0PBN0|C0PBN0_MAIZE	BZIP transcriptional activator RSG, putative, expressed	Q2QXC3	S130	9.2E-04	0.84	1.42		RH_{60}*		CL6		
tr|B6T559|B6T559_MAIZE	RING finger protein 126	B6T559	S93/S100	p/a	p/a	1.31		$RH_{5, 20, 30, 45, 60}$		CL7		

[a] Refers to UniProtKB Identifier retrieved from sequence similarity searches using the UniProt BLAST tool (http://www.uniprot.org/).

[b] Multiple sites of phosphorylation are separated by a coma while ambiguous sites are separated by /. All phosphorylation sites reported here were confirmed by manual inspection of the raw data to verify the phosphorylation site assignment obtained using X! Tandem.

[c] Refers to the *p* values obtained from the one-way ANOVA, "p/a" refers to qualitative changes.

[d] Refers to the fold change computed between the light to heavy ratio measured during MWD and the light to heavy ratio measured during $CTRL_1$. Decreasing trends in phosphopeptide abundance are highlighted in green while increasing trends in phosphopeptide abundance are highlighted in red.

[e] Refers to the fold change computed between the light to heavy ratio measured during SWD and the light to heavy ratio measured during $CTRL_2$. Decreasing trends in phosphopeptide abundance are highlighted in green whereas increasing trends in phosphopeptide abundance are highlighted in red.

[f] "> 50%" indicates that the ratio between quantitative changes relative to control plants detected on mild water deficit (MWD) and those detected on sever water deficit (SWD) reached more than 0.5.

[g] Refers to time points of the rehydration kinetics which displayed a >50% recovery compared to the variation of phosphopeptide abundances detected during SWD. "*" indicates when the linear regression of phosphopeptide abundances vs. duration of the rewatering events, was significant (p value < 0.05).

[h] Kendall τ coefficient refers to the correlation between relative abundance of phosphorylation site and midday leaf water potential. Only significant Kendall τ coefficients are showed (p value < 0.02). Plots are shown in supplemental Fig. S3.

[i] Refers to the cluster number shown in Fig. 5 and in supplemental Fig. S2.

[j] Refers to the fold change computed between the light to heavy ratio measured during SWD and the light to heavy ratio measured during $CTRL_2$ at the protein level. Information is provided for each reliably quantified protein, "ns" indicates that no significant change was detected. SWD-induced decreases in protein abundance are highlighted in green while SWD-induced increases in protein abundance are highlighted in red.

[k] Refers to the fold change computed between the light to heavy ratio measured during RH_{60} and the light to heavy ratio measured during SWD at the protein level. Information is provided for each reliably quantified protein, "ns" indicates that no significant change was detected. RH_{60}-induced decreases in protein abundance are highlighted in green while RH_{60}-induced increases in protein abundance are highlighted in red.

sucrose synthase 3, showed a significant quantitative variation between SWD and RH_{60} (Table I and supplemental Fig. S5), whereas this change was not observed in the phosphopeptide abundance. Overall, the abundance variations of phosphopeptides and nonphosphopeptides were consistent across $CTRL_2$, SWD and RH_{60} for only two proteins (a dehydrin COR410 and an auxin-repressed protein). Along with the early phosphoproteomic variations observed during the first minutes of rehydration, these results support the hypothesis that most of the detected phosphorylation changes was related to variations of the phosphorylation status rather than to variations of protein abundance. Likewise, several proteins displayed two or more phosphorylation sites that behaved differently, either changing/unchanging or belonging to differ-

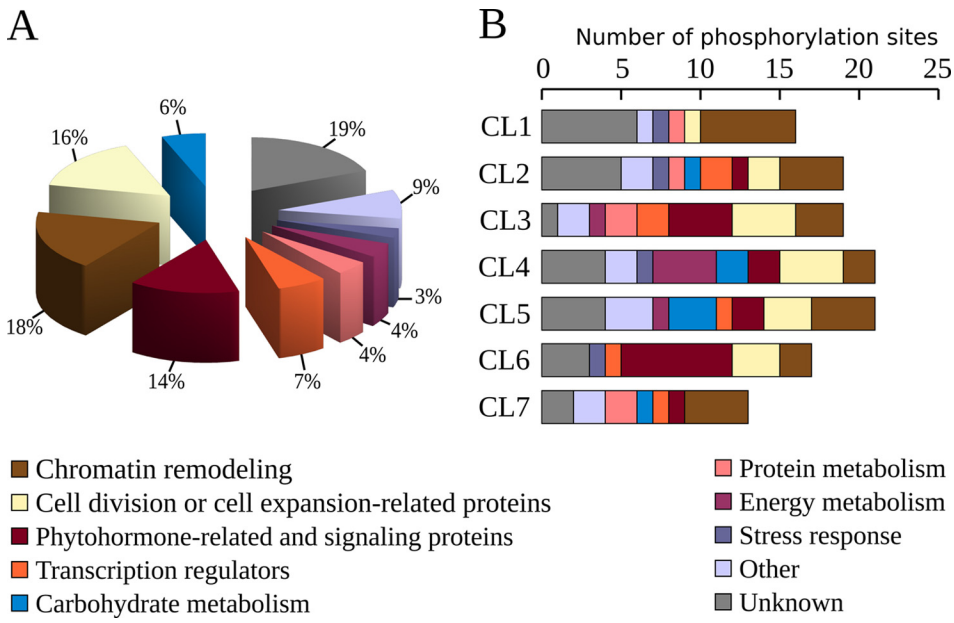

FIG. 4. **Functional cataloging of proteins displaying changing phosphorylation status in the growing zone of maize leaves upon contrasting water regimes.** *A*, proteins were functionally categorized using the UNIPROT database, the DBGET system or from information retrieved from already published works. *B*, the number of phosphorylation sites associated with the seven main SOTA clusters are shown according to their functional classification. The cluster identifications (CL1, CL2, CL3, CL4, CL5, CL6, and CL7) refer to Fig. 5 and Table I.

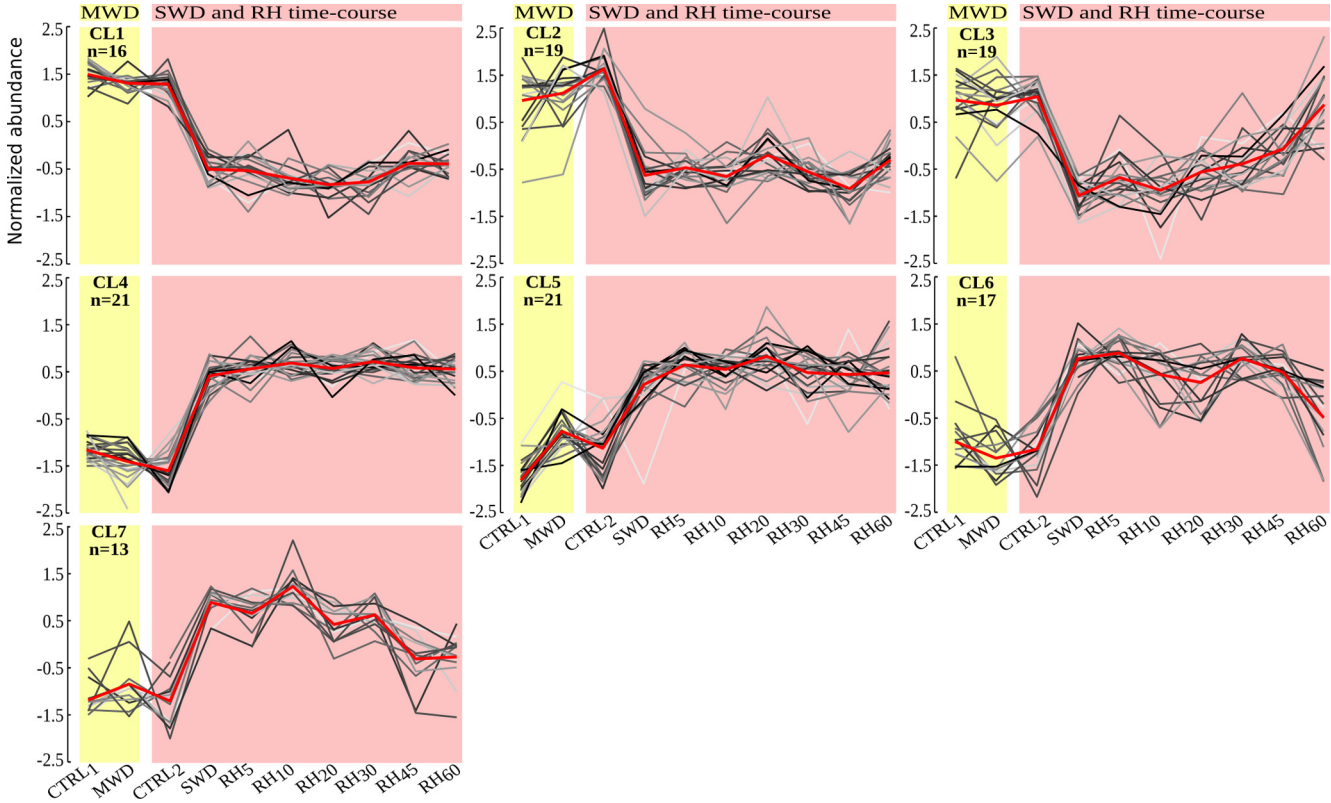

FIG. 5. **Self organizing tree algorithm (SOTA clustering) of the phosphorylation sites significantly affected by plant water status.** The seven main clusters are shown (the four additional clusters are displayed in supplemental Fig. S3). Individual profiles are depicted by *gray lines* (Z score) for mild water deficit (MWD), severe water deficit (SWD), and for the rehydration time course (RH_5 to RH_{60}), in comparison to control plants ($CTRL_1$ and $CTRL_2$) at the similar ontogenic development (for a detailed view of individual profiles, see supplemental Fig. S6). The average profile is marked in *red*. The cluster identification and the number of profiles included in each cluster are indicated in the left upper corner.

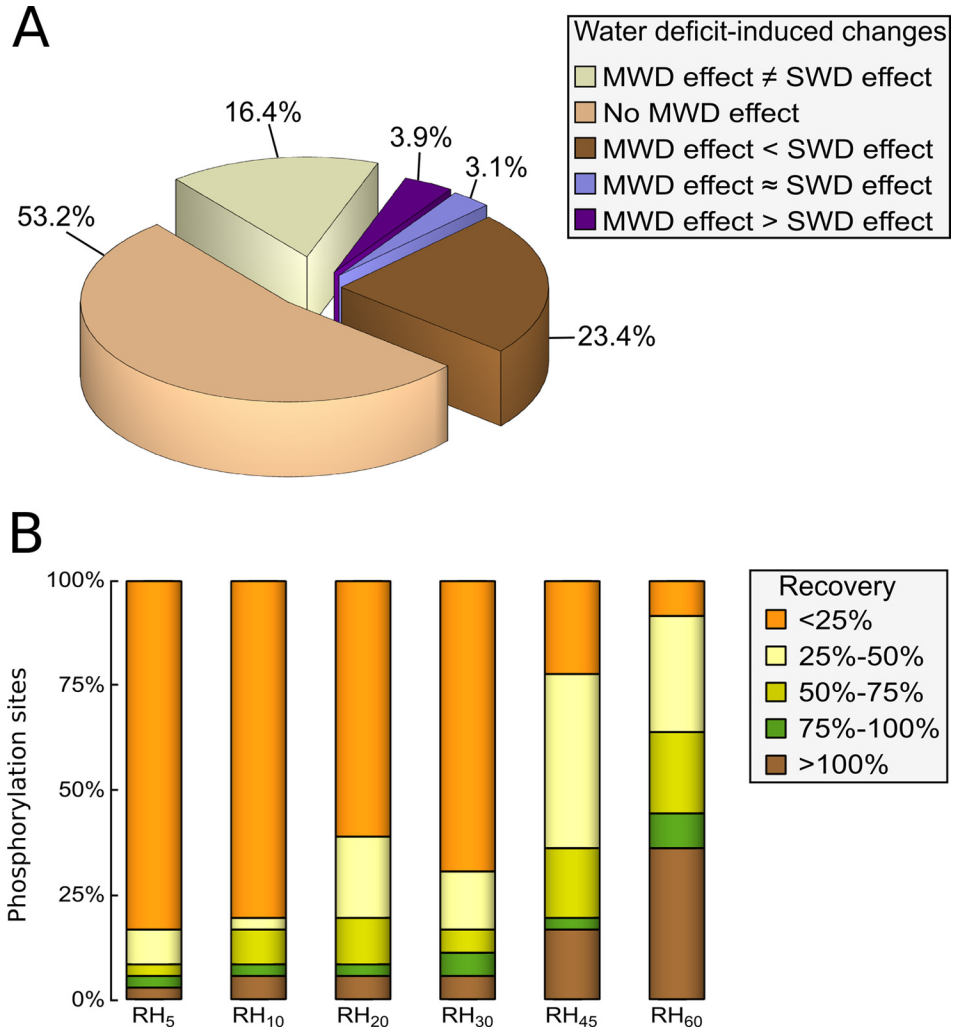

FIG. 6. **Contrasts between mild *versus* severe water deficit responses, and magnitude of the recoveries in protein phosphorylation status during the rehydration time course.** *A*, the distribution of phosphorylated peptides are shown according to the consistency/discrepancy of their changes in abundance detected upon mild water deficit (MWD) and compared with severe water deficit (SWD). Consistency/discrepancy criterion was assessed by computing the ratio between the quantitative changes relative to control plants detected upon MWD and those detected upon SWD. "MWD effect ≠ SWD effect": MWD induced antagonizing changes compared with those observed upon SWD; "No MWD effect": MWD did not induce any changes in protein phosphorylation status (MWD-induced changes were less than 25% of those detected upon SWD); "MWD effect < SWD effect": MWD-induced changes were of smaller magnitude compared with SWD-induced changes (ranging from 25% to 75% of those detected upon SWD); "MWD effect ≈ SWD effect": changes of comparable magnitude were observed regardless of the water deficit intensity (MWD-induced changes reached 75% to 125% of those detected upon SWD); "MWD effect > SWD effect": MWD induced changes of larger magnitude compared with SWD-induced changes (more than 125% of those observed upon SWD). *B*, for each rehydration time point (RH_5, RH_{10}, RH_{20}, RH_{30}, RH_{45}, and RH_{60}), the magnitude of the recovery in protein phosphorylation status is indicated for the 36 phosphorylation sites displaying a significant linear regression between phosphopeptide abundance and the duration of the rehydration.

ent clusters (*e.g.* S312/S313 and S241 in a GTP-ase activating protein for Arf containing protein, S177 and S166 in a putative uncharacterized protein; Table I and supplemental Table S3). Contrasting phosphorylation dynamics occurring on different sites within the same protein cannot be explained by a variation of protein abundance as well. In addition, such independent variations at different sites of the same protein emphasize that different phosphorylation events have specific roles (31).

DISCUSSION

In this study, we report the first analysis of the phosphorylation dynamics in the growing zone of leaves that resolves an *in vivo* time course of dehydration and rehydration. Quantitative changes of protein phosphorylation status were evaluated during an early and mild water deficit (MWD), and a severe water deficit (SWD) both impacting plant growth in comparison with constant optimal watering at the same ontogenic stage ($CTRL_1$ and $CTRL_2$, respectively). Phosphoproteome

changes were also analyzed in comparison with SWD, over a time course of recovery periods lasting 5, 10, 20, 30, 45, and 60 min (RH_5, RH_{10}, RH_{20}, RH_{30}, RH_{45}, and RH_{60}, respectively) that induced partial recovery of the midday leaf water potential. As leaf elongation rate recovers faster than leaf water potential (22), reactivation of plant growth processes was likely to occur within the duration of the studied rehydration kinetics.

Phosphoproteomics of the Growing Zone of Leaves Evidences In Vivo Covariations Between Protein Phosphorylation Events and Plant Water Status—In the growing zone of maize leaves, the length of the zone with cell division is close to 70 mm in the sixth leaf and lengthens in younger leaves (10). Within this range, cell division rate is maximum in the first 20 mm and decreases along with the distance to the leaf insertion point, overlapping in space with expanding cells. This means that our analysis, carried out on a 5 cm-long leaf fragment, provides a picture of phosphorylation events occurring in tissues where both cell division and expansion happen. Upon water deficit, cell division rate is affected all along the growing zone, and cell expansion is altered approximately to the same extent (32). Thus, phosphopeptide variations observed between controls and WD samples should not be primarily related to the variation of the ratio between dividing and expanding cells. The variation of this ratio is even less expected to occur during the short period of rehydration.

Using quantitative phosphoproteomics, we identified 138 phosphorylation sites that were altered upon changing plant water statuses in the leaf growing zone. Interestingly, 75% of the changes referring to proteins of known functions, belonged to five main processes directly or indirectly involved in the regulation of plant development, either through epigenetic and transcriptional regulations, cell cycle-related changes, hormone-mediated responses or carbohydrate metabolism adjustments (Fig. 7).

In this study, MWD exemplified the first stage of the growth decrease when leaf water potential was not altered yet. Therefore, the similar changes in phosphorylation status observed in both MWD and SWD could correspond to early responses which were maintained over the establishment of water deficit, whereas the changes of lower magnitude suggest that part of the variations could depend on the duration and/or on the intensity of water shortage. On the contrary, the changes of higher magnitude or opposite to those detected during SWD, reveal specific responses of the early stage of water stress response. Our findings also emphasize rapid events in protein phosphorylation occurring *in vivo* within minutes, during early changes in plant water status. The picture of these rapid phosphorylation events, that were basically observed during the rehydration kinetics, evidenced that the earliest phosphorylation events mainly concerned cell cycle-related proteins. This emphasizes that the regulation of the cell cycle-related processes are among the primary targets of the phosphorylation and dephosphorylation machinery. Early changes in the phosphorylation status of cell cycle-related proteins could sustain the rapid recovery of leaf growth occurring within minutes in maize (22).

Transitory phosphorylation/dephosphorylation events in the range of 10 to 30 min after rewatering were mainly observed for kinases and phosphatases, including hormone-related proteins (Fig. 7). This could be a consequence of the recovery of water fluxes and turgor in the leaf, which was likely to occur concomitantly with the recovery of leaf water potential. These phosphorylation events detected on kinase and phosphatase proteins could act within signaling cascades, in an upstream control of further changes detected later during the rehydration time-course. On the contrary, no change was detected in kinases or phosphatases within 5 min rehydration although signaling events are rather expected at an early stage upon changing environments, and despite the identification, as early as 5 min after watering, of changing phosphorylation statuses of proteins involved in other functional processes. Inherently to exploratory phosphoproteomics approaches, some fine-tuned events were probably not detected in this study.

Fully or partially reversible events were also widely observed in the phosphorylation status of proteins related to epigenetic and transcriptional regulation (Fig. 7), which is consistent with the fact that the cell cycle-related changes require extensive epigenetic and transcriptional regulations for achieving cell cycle transitions, as already reported in growing organs of *Arabidopsis thaliana* plants (33, 34). In contrast, the phosphorylation events occurring in carbohydrate metabolism-related proteins, appeared rather as sustainable changes over the whole rehydration time course (Fig. 7).

As a whole, the dependence on stress intensity, the significant correlations with plant water status as well as the rapid recoveries observed during rehydration, collectively suggest that a substantial part of the observed phosphorylation dynamics are of functional relevance in the response of maize leaves to contrasting water regimes.

Earliest Changes in Plant Water Status Involve Cytokinesis- and Cell Expansion-related Proteins—The cell cycle is likely to encounter substantial changes in response to adverse environmental conditions (8–10). In many plant organs, including leaves, roots and seeds, water deficit rapidly decreases cell division rate (4, 7, 35). In this study, 19 changes in phosphorylation status involved proteins acting in cell cycle-related processes (Fig. 7). These proteins are likely involved in a general control of the cell cycle (*i.e.* USP family proteins, calmodulin binding protein and calmodulin), in the phragmoplast and the nuclear envelope assembly (*i.e.* vacuolar protein sorting 26, nuclear matrix constituent protein 1, pollen-specific protein, villin-3, MAP65–1a microtubule-associated protein, CLIP-associating protein 1, and kinesin), and in the cell plate initiation and maturation (*i.e.* Arf-GTPase, epsin, adaptin, Golgi-SNARE 12 protein, and AIR9). Although previous

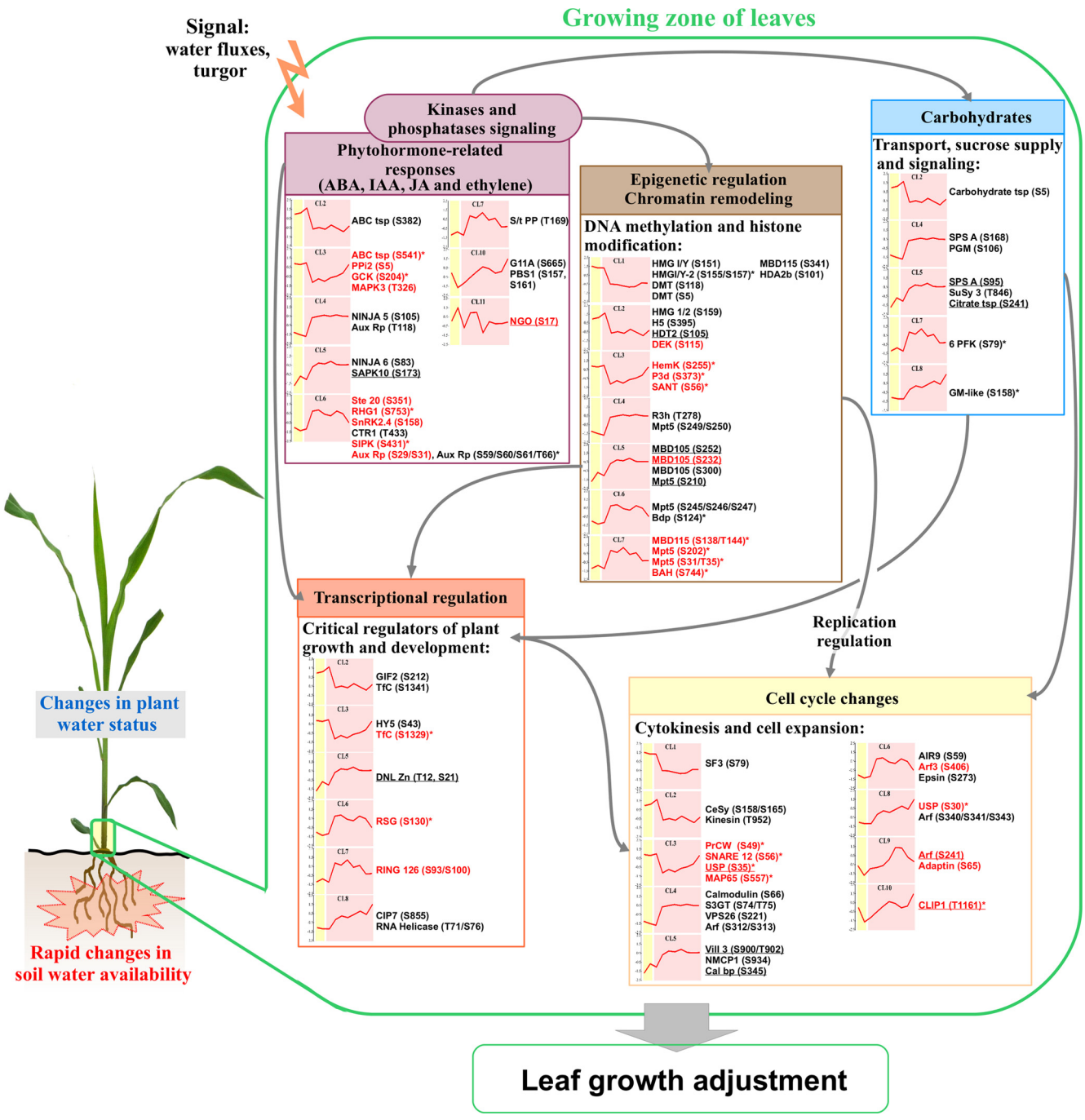

FIG. 7. **Overview of the main processes involving proteins whose phosphorylation status was rapidly altered in response to changing plant water statuses in the growing zone of maize leaves.** The five main processes identified in this study are shown. Graphs refer to the SOTA clusters shown in Fig. 5, only the average profile is depicted in *red*. Individual profiles are shown in supplemental Fig. S6. Proteins displaying at least one phosphopeptide belonging to any SOTA clusters are indicated. Underlined proteins show that mild water deficit (MWD) induced at least half of the change in phosphopeptide abundance that was detected during severe water deficit (SWD). Proteins depicted in *red* show that 5, 10, 20, 30, 45, or 60 min rehydration (RH_5, RH_{10}, RH_{20}, RH_{30}, RH_{45}, or RH_{60}, respectively) enabled at least a half recovery and * indicates when the linear regression of phosphopeptide abundances *versus* duration of the rewatering events, was significant (p value < 0.05). *Arrows* refer to functional links between processes. Abbreviations: ABA, abscisic acid; IAA, auxin; JA, jasmonic acid; ABC tsp, MDR-like ABC transporter; PPi2, protein phosphatase inhibitor 2; GCK, GCK-like kinase MIK; MAPK3, Map3k delta-1 protein kinase; NINJA, novel Interactor of JAZ-family proteins; Aux Rp, auxin-repressed protein; SAPK10, serine/threonine-protein kinase SAPK10; Ste 20, Ste-20 related kinase; RHG1, receptor-like kinase RHG1; SnRK, sucrose nonfermenting related kinase; CTR1, serine/threonine-protein kinase ctr1; SIPK, salt-inducible protein kinase; S/t PP, Serine/threonine-protein phosphatase; G11A, protein kinase G11A; PBS1, Serine/threonine-protein kinase PBS1; NGO, naringenin,2-oxoglutarate 3-dioxygenase; HMG, high mobility group protein; DMT, DNA (cytosine-5)-methyltransferase 1;

studies mainly reported the impact of water deficit in delaying the G1-to-S transition as a result of a reduced cyclin-dependent kinase activity (5, 36), here we identified quantitative changes of phosphoproteins involved in the mitosis phase and in cytokinesis.

Another evidence of changes in growth-related processes was the identification of phosphoproteins involved in cell wall biogenesis and remodeling, because both processes of cytokinesis and cell expansion require the addition of new cell wall components (37, 38). Here, we identified three altered phosphosites belonging to a cellulose synthase, a proline-rich cell wall protein (two proteins involved in cell wall building), and a sterol glycosyltransferase providing sterolglycosides which can act as precursors for cellulose biosynthesis. Another change was observed in a sucrose synthase which could be involved in the synthesis of cell wall components by providing UDP-glucose directly to the cellulose synthases and/or callose synthases (39).

Recovery of Leaf Water Potential Mainly Matches With Hormone-mediated Responses and Cell Signaling Events—Plant hormones are major regulators of growth and development, and they rapidly affect many aspects of plant biology during responses to biotic and abiotic stresses (40, 41). For instance, abscisic acid, jasmonate, and ethylene have already been reported as critical regulators of the early plant growth adjustments during drought or osmotic stress (14, 15). Here, we identified ten sites with significant changes in phosphorylation status belonging to proteins involved in either ABA-, ethylene-, auxin- or jasmonate-related responses. Our study evidenced single sites in two kinase proteins, SAPK10 and SnRK2.4, both belonging to the SnRK2 family proteins which play a pivotal role in regulating sucrose metabolism, several ion channels and ABA-induced gene expression (42, 43). Interestingly, the phosphorylation status of SnRK2.4 transiently recovered to the control level in the range of 10 to 20 min after rewatering. A rapid phosphorylation increase has already been observed in SnRK2 family proteins following 30-min ABA treatment (19). A slight and transitory recovery was also identified during 10 to 20 min rewatering for a phosphopeptide of Ctr1, a Raf-like protein kinase acting as the main negative regulator of the ethylene signal transduction chain. This is an interesting finding because ethylene has recently been reported as an early upstream regulator of the cell cycle machinery (15). Regarding auxin-related proteins, two drought-induced phosphorylation changes recovered in two auxin-repressed proteins (one recovered after 60 min rewatering whereas the other one was correlated with the recovery of plant water status). Finally, two increasing phosphorylated forms were detected in NINJA-family proteins 5 and 6 (Novel Interactor of JAZ-family proteins). NINJA is a member of the ABI five binding proteins that interact with the Jasmonate ZIM-domain proteins (JAZ proteins) for repressing jasmonate response genes (44).

Furthermore, we evidenced phosphorylation events in seven additional protein kinases and two phosphatases, named G11A, PBS1, Ste-20 related kinase, Map3k delta-1, GCK-like kinase MIK, salt-inducible protein kinase (SIPK), receptor-like kinase RHG1, protein phosphatase inhibitor 2 containing protein, and a serine/threonine-protein phosphatase, although little information is available for most of them. GCK MIK is believed to play a role in plant growth and development. Belonging to the GCK subgroup of MAP4Ks, it interacts with the maize atypical receptor kinase (MARK), a receptor expressed during embryogenesis and in the meristems of maize (45). Noteworthy, phosphorylation changes in the Ste-20 related kinase, in the Map3k delta-1 protein kinase, in SIPK and in RHG1 displayed transient recoveries after 20 min rewatering.

Changes in Plant Water Status Induce Reversible Modifications Preparing Epigenetic and Transcriptional Regulations—Up to 25% of the phosphorylation sites displaying significant changes in response to water regimes belonged to proteins involved in an upstream control of gene expression, mainly influencing chromatin structure and transcriptional regulation. Here, significant changes were observed in 25 phosphorylation sites belonging to proteins directly or indirectly involved in histone modification and DNA methylation. In response to environmental cues, gene expression and plant development are influenced by extensive chromatin remodeling, mainly achieved through histone post-translational modifications or DNA methylation patterns (46). Likewise, specific chromatin modifications occurring at both histone and DNA levels are also a prerequisite to sustain the transcriptional regulation involved in the cell cycle progression (33, 47). In this study, decreased phosphorylated forms in response to dehydration were detected in 12 phosphorylation sites belonging to proteins acting on chromatin structure or in DNA

H5, histone H5; HDT2, histone deacetylase HDT2; DEK, protein DEK; MBD105/115, methyl-binding domain protein 105/115; HDA2b, Histone deacetylase 2b; HemK, methyltransferase family member 2; P3d, plus-3 domain containing protein; SANT, SANT DNA-binding protein; R3h, R3h domain containing protein; Mpt5, pumilio/Mpt5 family RNA-binding protein; Bdp, Bromodomain-containing protein; BAH, bromo-adjacent homology (BAH) domain-containing protein; Carbohydrate tsp, carbohydrate transporter/sugar porter/transporter; SPS A, sucrose phosphate synthase A; PGM, phosphoglucomutase; SuSy 3, sucrose synthase 3; Citrate tsp, citrate transporter family protein; 6 PFK, 6-phosphofructokinase; GM-like, galactose mutarotase-like; GIF2, GRF-interacting factor GIF2; TfC, protein TIME FOR COFFEE; HY5, LONG HYPOCOTYL 5 bZIP transcription factor; DNL Zn, DNL zinc finger family protein; RSG, bZIP transcriptional activator RSG; RING 126, RING finger protein 126; CIP7, COP1-interacting protein 7; SF3, pollen-specific protein SF3; AIR9, microtubule-associated protein *AIR9*; Arf, ADP-ribosylation factor GTPase-activating protein; CeSy, cellulose synthase-2; USP, universal stress protein; PrCW, proline-rich cell wall protein; SNARE 12, golgi SNARE 12 protein; MAP65, microtubule-associated protein MAP65–1a; S3GT, sterol 3-beta-glucosyltransferase; VPS26, vacuolar protein sorting 26; CLIP1, CLIP-associating protein 1; Vill 3, villin-3; NMCP1, nuclear matrix constituent protein 1; Cal bp, calmodulin binding protein.

methylation (Fig. 7). Partial or full recoveries were observed for five of them, including a small chromatin-associated proteins (HMG I/Y-2), a DEK protein (a nuclear chromatin-associated phosphoprotein (48), a SANT domain- (a histone-interaction module (49)), a plus-3 domain-containing proteins, and a HemK protein (a class of methyl transferase proteins). Furthermore, increased phosphorylation upon SWD was evidenced in 11 phosphorylation sites belonging to seven proteins. Partial or full recoveries were observed for six of them, including two sites of a Pumilio/MPT5 proteins and single sites belonging to a MBD105 proteins, a MBD115 protein, a bromodomain- and a BAH domain- containing proteins. BAH and bromodomains are structural motifs commonly found in chromatin-associated proteins that recognize methylated and acetylated lysine residues, respectively. Their phosphorylation changes were concomitant to those observed on DNA methylation or histone deacetylation-related proteins.

Along with these nuclear architectural events changing the overall DNA accessibility, significant modifications of five critical regulators of plant growth and development were evidenced, including single sites in a GRF-interacting factor GIF2, in a bZIP transcriptional activator RSG (for repression of shoot growth), in a COP1-interacting protein 7 (CIP7), in a LONG HYPOCOTYL 5 bZIP transcription factor (HY5) and two sites in a TIME FOR COFFEE protein (TIC). GIF genes act in organ size control through a possible role in cell proliferation by positively regulating cell-cycle gene expression (50, 51) and RSG is involved in cell elongation by controlling the endogenous amounts of gibberellins (52). The function of RSG is known to be negatively regulated by 14–3-3 proteins that bind to RSG depending on its phosphorylation status, thereby sequestering RSG in the cytoplasm and making it unable to regulate its targets in the nucleus (53). These results suggest that the above processes may trigger further changes in cell division and expansion under water deficit. Likewise, TIC is a nuclear regulator of the circadian clock and could control various aspects of hormone-related processes involved in plant growth and development (54). CIP7 and HY5 are pivotal regulators of plant photomorphogenic development and both are interactors of COP1 (55). Being required for hypocotyl inhibition in all light conditions, HY5 is linked to a wide range of processes involving auxin, jasmonate, abscissic acid, ethylene and gibberellins pathways (56) which is in agreement with the hormone-mediated responses that have already been suggested above. CIP7 is a negative regulator of COP1 whereas this latter is a direct repressor of HY5 by inducing its proteasome-mediated degradation, resulting in the reduced expression of photomorphogenic genes (56, 57). Previous experiments suggested a role of HY5 phosphorylation in changing COP1-HY5 interaction.

Phosphorylation Changes Related to Carbohydrate Metabolism Refer to Long-term Adjustments—Phosphorylation changes occurring in proteins involved in carbohydrate metabolism accounted for a minor part of the whole detected variations, although sugars are major metabolites involved in stress responses. Glucose and especially sucrose can act as signaling molecules influencing the expression of a wide spectrum of genes and as the most suitable source of carbon and energy for many aspects of plant growth and development (58). In response to contrasting water regimes, two phosphopeptides of a sucrose phosphate synthase (SPS) and single phosphopeptides in a sucrose synthase (SuSy), in a phosphoglucomutase (PGM), in a phosphofructokinase (PFK), in a carbohydrate transporter and in a citrate transporter displayed significant changes in relative abundance. SPS phosphorylation occurs on multiple seryl residues *in vivo* and involves SnRK protein kinases at least (43, 59), which is in agreement with the rapid changes in the two SnRK2 proteins, described above. Changes in SPS activity during osmotic stress have already been observed as a consequence of phosphorylation events that differently occur on different sites (59). Here, except for the site identified in the carbohydrate transporter, detected phosphorylation sites were overall increased during SWD, with a partial recovery during rehydration for PFK only. Our results suggest long-term changes in the sucrose supply through phosphorylation events in both SPS and SuSy, but also in PGM and PFK which provide substrates for sucrose synthesis.

In conclusion, by combining physiological characterizations with phosphoproteome analysis, we reported here the first phosphoproteome dynamics occurring *in vivo* in the growing zone of maize leaves upon rapid changes in plant water status. Severe water deficit deeply modified the phosphorylation status of proteins, and part of these modifications was observed early, *i.e.* at a time when leaf water potential and plant growth were only slightly affected. During rehydration, that enables leaf growth resumption, this work enabled to identify transitory phosphorylation events as well as rapid *in vivo* changes occurring within five to 10 min after watering, independently to protein abundance variations. This exploratory approach emphasizes a comprehensive picture of the molecular plasticity of the phosphoproteome of leaf growing tissues upon dehydration/rehydration, and reveals a number early protein targets of the phosphorylation/dephosphorylation process potentially involved in an upstream control of the rapid leaf growth adjustment. This provides first insights into the *in vivo* dynamic behavior of individual protein phosphorylation sites upon changing plant water statuses. These findings are meant to guide future research on early plant water stress responses and on the understanding of processes involved in the rapid growth adjustment occurring upon fluctuating plant water status.

Acknowledgments—We thank Edlira Nano for her excellent technical assistance in the use of the MassChroQ software and to Olivier Langella for making LC-MS/MS data available in the PROTICdb database. We gratefully acknowledge Delphine Pflieger for her careful reading and editing of this manuscript. We also acknowledge Attila

Csordas, from the PRIDE staff, for his excellent technical assistance in MS data submission.

* This research work was supported by a grant from the Agence National de la Recherche (DROMADAiR project, 08-GENM-003).

S This article contains supplemental Figs. S1 to S6 and Tables S1 to S3.

‖ To whom correspondence should be addressed: INRA/University Paris-Sud/CNRS/AgroParisTech, UMR 0320/UMR 8120 Génétique Végétale, Gif-sur-Yvette, 91190, France. E-mail: ludovic.bonhomme@univ-evry.fr or zivy@moulon.inra.fr.

REFERENCES

1. Chaves, M. M., Maroco, J. P., and Pereira, J. S. (2003) Understanding plant responses to drought - from genes to the whole plant. *Func. Plant Biol.* **30,** 239–264
2. Saab, I. N., and Sharp, R. E. (1989) Non-hydraulic signals from maize roots in drying soil: inhibition of leaf elongation but not stomatal conductance. *Planta.* **179,** 466–474
3. Westgate, M. E., and Boyer, J. S. (1985) Osmotic adjustment and the inhibition of leaf, root, stem and silk growth at low water potentials in maize. *Planta* **164,** 540–549
4. Tardieu, F., and Granier, C. (2011) Water deficit and growth. Co-ordinating processes without an orchestrator? *Curr. Opin. Plant Biol.* **14,** 283–289
5. Granier, C., and Tardieu, F. (1999) Water deficit and spatial pattern of leaf development. Variability in responses can be simulated using a simple model of leaf development. *Plant Physiol.* **119,** 609–620
6. Ben-Haj-Salah, H., and Tardieu, F. (1995) Temperature affects expansion rate of maize leaves without change in spatial distribution of cell length (Analysis of the coordination between cell division and cell expansion). *Plant Physiol.* **109,** 861–870
7. Skirycz, A., and Inzé, D. (2010) More from less: plant growth under limited water. *Curr. Opin. Biotech.* **21,** 197–203
8. Schuppler, U., He, P. H., John, P. C., and Munns, R. (1998) Effect of water stress on cell division and cell-division-cycle 2-like cell-cycle kinase activity in wheat leaves. *Plant Physiol.* **117,** 667–678
9. Aguirrezabal, L., Bouchier-Combaud, S., Radziejwoski, A., Dauzat, M., Cookson, S. J., and Granier, C. (2006) Plasticity to soil water deficit in *Arabidopsis thaliana*: dissection of leaf development into underlying growth dynamic and cellular variables reveals invisible phenotypes. *Plant Cell Environ.* **29,** 2216–2227
10. Granier, C., Inzé, D., and Tardieu, F. (2000) Spatial distribution of cell division rate can be deduced from that of p34(cdc2) kinase activity in maize leaves grown at contrasting temperatures and soil water conditions. *Plant Physiol.* **124,** 1393–1402
11. Cosgrove, D. J. (2005) Growth of the plant cell wall. *Nat. Rev. Mol. Cell Biol.* **6,** 850–861
12. Vincent, D., Lapierre, C., Pollet, B., Cornic, G., Negroni, L., and Zivy, M. (2005) Water deficits affect caffeate O-methyltransferase, lignification, and related enzymes in maize leaves. A proteomic investigation. *Plant Physiol.* **137,** 949–960
13. Muller, B., Bourdais, G., Reidy, B., Bencivenni, C., Massonneau, A., Condamine, P., Rolland, G., Conéjéro, G., Rogowsky, P., and Tardieu, F. (2007) Association of specific expansins with growth in maize leaves is maintained under environmental, genetic, and developmental sources of variation. *Plant Physiol.* **143,** 278–290
14. Harb, A., Krishnan, A., Ambavaram, M. M., and Pereira, A. (2010) Molecular and physiological analysis of drought stress in *Arabidopsis* reveals early responses leading to acclimation in plant growth. *Plant Physiol.* **154,** 1254–1271
15. Skirycz, A., Claeys, H., De Bodt, S., Oikawa, A., Shinoda, S., Andriankaja, M., Maleux, K., Eloy, N. B., Coppens, F., Yoo, S. D., Saito, K., and Inzé, D. (2011) Pause-and-stop: the effects of osmotic stress on cell proliferation during early leaf development in *Arabidopsis* and a role for ethylene signaling in cell cycle arrest. *Plant Cell.* **23,** 1876–1888
16. Novak, B., Kapuy, O., Domingo-Sananes, M. R., and Tyson, J. J. (2010) Regulated protein kinases and phosphatases in cell cycle decisions. *Curr. Opin. Cell Biol.* **22,** 801–808
17. Schulze, W. X. (2010) Proteomics approaches to understand protein phosphorylation in pathway modulation. *Curr. Opin. Plant Biol.* **13,** 279–286
18. Niittylä, T., Fuglsang, A. T., Palmgren, M. G., Frommer, W. B., and Schulze, W. X. (2007) Temporal analysis of sucrose-induced phosphorylation changes in plasma membrane proteins of Arabidopsis. *Mol. Cell. Proteomics.* **6,** 1711–1726
19. Kline, K. G., Barrett-Wilt, G. A., and Sussman, M. R. (2010) In planta changes in protein phosphorylation induced by the plant hormone abscisic acid. *Proc. Natl. Acad. Sci. U.S.A.* **107,** 15986–15991
20. Ke, Y., Han, G., He, H., and Li, J. (2009) Differential regulation of proteins and phosphoproteins in rice under drought stress. *Biochem. Biophys. Res. Commun.* **379,** 133–138
21. Röhrig, H., Schmidt, J., Colby, T., Bräutigam, A., Hufnagel, P., and Bartels, D. (2006) Desiccation of the resurrection plant *Craterostigma plantagineum* induces dynamic changes in protein phosphorylation. *Plant Cell Environ.* **29,** 1606–1617
22. Parent, B., Hachez, C, Redondo, E., Simonneau, T., Chaumont, F., and Tardieu, F. (2009) Drought and abscisic acid effects on aquaporin content translate into changes in hydraulic conductivity and leaf growth rate: a trans-scale approach. *Plant Physiol.* **149,** 2000–2012
23. Méchin, V., Damerval, C., and Zivy, M. (2007) *Plant Proteomics: Methods and Protocols*, pp 1–8, Humana Press, Totowa, New Jersey, U.S.A.
24. Boersema, P. J., Raijmakers, R., Lemeer, S., Mohammed, S., and Heck, A. J. R. (2009) Multiplex peptide stable isotope dimethyl labeling for quantitative proteomics. *Nat. Protoc.* **4,** 484–494
25. Nühse, T. S., Bottrill, A. R., Jones, A. M., and Peck, S. C. (2007) Quantitative phosphoproteomic analysis of plasma membrane proteins reveals regulatory mechanisms of plant innate immune responses. *Plant J.* **51,** 931–940
26. Valot, B., Langella, O., Nano, E., and Zivy, M. (2011) MassChroQ: A versatile tool for mass spectrometry quantification. *Proteomics*. **17,** 3572–3577.
27. Ferry-Dumazet, H., Houel, G., Montalent, P., Moreau, L., Langella, O., Negroni, L., Vincent, D., Lalanne, C., de Daruvar, A., Plomion, C., Zivy, M., and Joets, J. (2005) PROTICdb: a web-based application to store, track, query, and compare plant proteome data. *Proteomics.* **5,** 2069–2081
28. Storey, J. D., and Tibshirani, R. (2003) Statistical significance for genome-wide studies. *Proc. Natl. Acad. Sci. U.S.A.* **100,** 9440–9445
29. Sperry, J. S., Hacke, U. G., Oren, R., and Comstock, J. P. (2002) Water deficits and hydraulic limits to leaf water supply. *Plant Cell Environ.* **25,** 251–263
30. Boersema, P. J., Foong, L. Y., Ding, V. M., Lemeer, S., van Breukelen, B., Philp, R., Boekhorst, J., Snel, B., den Hertog, J., Choo, A. B., and Heck, A. J. R. (2010) In-depth qualitative and quantitative profiling of tyrosine phosphorylation using a combination of phosphopeptide immunoaffinity purification and stable isotope dimethyl labeling. *Mol. Cell. Proteomics.* **9,** 84–99
31. Olsen, J. V., Blagoev, B., Gnad, F., Macek, B., Kumar, C., Mortensen, P., and Mann, M. (2006) Global, *in vivo*, and site-specific phosphorylation dynamics in signaling networks. *Cell.* **127,** 635–648
32. Tardieu, F., Reymond, M., Hamard, P., Granier, C., and Muller, B. (2000) Spatial distributions of expansion rate, cell division rate and cell size in maize leaves: a synthesis of the effects of soil water status, evaporative demand and temperature. *J. Exp. Bot.* **51,** 1505–1514
33. Beemster, G. T., De Veylder, L., Vercruysse, S., West, G., Rombaut, D., Van Hummelen, P., Galichet, A., Gruissem, W., Inzé, D., and Vuylsteke, M. (2005) Genome-wide analysis of gene expression profiles associated with cell cycle transitions in growing organs of *Arabidopsis*. *Plant Physiol.* **138,** 734–743
34. Desvoyes, B., Sanchez, M. P., Ramirez-Parra, E., and Gutierrez, C. (2010) Impact of nucleosome dynamics and histone modifications on cell proliferation during *Arabidopsis* development. *Heredity*. **105,** 80–91
35. Stals, H., and Inzé, D. (2001) When plant cells decide to divide. *Trends Plant Sci.* **6,** 359–364
36. Inzé, D., and De Veylder, L. (2006) Cell cycle regulation in plant development. *Annu. Rev. Genet.* **40,** 77–105
37. Backues, S. K., Konopka, C. A., McMichael, C. M., and Bednarek, S. Y. (2007) Bridging the divide between cytokinesis and cell expansion. *Curr. Opin. Plant Biol.* **10,** 607–615
38. Jürgens, G. (2005) Cytokinesis in higher plants. *Annu. Rev. Plant Biol.* **56,** 281–299
39. Amor, Y., Haigler, C. H., Johnson, S., Wainscott, M., and Delmer, D. P. (1995) A membrane-associated form of sucrose synthase and its poten-

tial role in synthesis of cellulose and callose in plants. *Proc. Natl. Acad. Sci. U.S.A.* **92,** 9353–9357
40. Santner, A., Calderon-Villalobos, L. I., and Estelle, M. (2009) Plant hormones are versatile chemical regulators of plant growth. *Nat. Chem. Biol.* **5,** 301–307
41. Wasternack, C. (2007) Jasmonates: an update on biosynthesis, signal transduction and action in plant stress response, growth and development. *Ann. Bot.* **100,** 681–697
42. Christmann, A., Moes, D., Himmelbach, A., Yang, Y., Tang, Y., and Grill, E. (2006) Integration of abscisic acid signalling into plant responses. *Plant Biol.* **8,** 314–325
43. Zheng, Z., Xiaoping, X., Crosley, R. A., Greenwalt, S. A., Sun, Y., Blakeslee, B., Wang, L., Ni, W., Sopko, M. S., Yao, C., Yau, K., Burton, S., Zhuang, M., McCaskill, D. G., Gachotte, D., Thompson, M., and Greene, T. W. (2010) The protein kinase SnRK2.6 mediates the regulation of sucrose metabolism and plant growth in *Arabidopsis*. *Plant Physiol.* **153,** 99–113
44. Pauwels, L., Barbero, G. F., Geerinck, J., Tilleman, S., Grunewald, W., Pérez, A. C., Chico, J. M., Bossche, R. V., Sewell, J., Gil, E., García-Casado, G., Witters, E., Inzé, D., Long, J. A., De Jaeger, G., Solano, R., and Goossens, A. (2010) NINJA connects the co-repressor TOPLESS to jasmonate signalling. *Nature.* **464,** 788–791
45. Llompart, B., Castells, E., Río, A., Roca, R., Ferrando, A., Stiefel, V., Puigdomenech, P., and Casacuberta, J. M. (2003) The direct activation of MIK, a germinal center kinase (GCK) -like kinase, by MARK , a maize atypical receptor kinase, suggests a new mechanism for signaling through kinase-dead receptors. *J. Biol. Chem.* **278,** 48105–48111
46. Chinnusamy, V., and Zhu, J. K. (2009) Epigenetic regulation of stress responses in plants. *Curr. Opin. Plant Biol.* **12,** 133–139
47. Sanchez, Mde, L., Caro, E., Desvoyes, B., Ramirez-Parra, E., and Gutierrez, C. (2008) Chromatin dynamics during the plant cell cycle. *Semin. Cell. Dev. Biol.* **19,** 537–546
48. Kappes, F., Scholten, I., Richter, N., and Gruss, C. (2004) Functional domains of the ubiquitous chromatin protein DEK. *Mol. Cell. Biol.* **24,** 6000–6010
49. Boyer, L., and Latek, R. (2004) The SANT domain: a unique histone-tail-binding module? *Nat. Rev. Mol. Cell.* **5,** 1–6
50. Kim, J. H., Choi, D., and Kende, H. (2003) The AtGRF family of putative transcription factors is involved in leaf and cotyledon growth in *Arabidopsis. Plant J.* **36,** 94–104
51. Lee, B. H., Ko, J. H., Lee, S., Lee, Y., Pak, J. H., and Kim, J. H. (2009) The *Arabidopsis* GRF-INTERACTING FACTOR gene family performs an overlapping function in determining organ size as well as multiple developmental properties. *Plant Physiol.* **151,** 655–668
52. Fukazawa, J., Sakai, T., Ishida, S., Yamaguchi, I., Kamiya, Y., and Takahashi, Y. (2000) Repression of shoot growth, a bZIP transcriptional activator, regulates cell elongation by controlling the level of gibberellins. *Plant Cell.* **12,** 901–915
53. Igarashi, D., Ishida, S., Fukazawa, J., and Takahashi, Y. (2001) 14-3-3 proteins regulate intracellular localization of the bZIP transcriptional activator RSG. *Plant Cell.* **13,** 2483–2497
54. Ding, Z., Millar, A. J., Davis, A. M., and Davis, S. J. (2007) TIME FOR COFFEE encodes a nuclear regulator in the *Arabidopsis thaliana* circadian clock. *Plant Cell.* **19,** 1522–1536
55. Yi, C., and Deng, X. W. (2005) COP1 – from plant photomorphogenesis to mammalian tumorigenesis. *Trends Cell Biol.* **15,** 618–625
56. Nemhauser, J. L. (2008) Dawning of a new era: photomorphogenesis as an integrated molecular network. *Curr. Opin. Plant Biol.* **11,** 4–8
57. Lee, J., He, K., Stolc, V., Lee, H., Figueroa, P., Gao, Y., Tongprasit, W., Zhao, H., Lee, I., and Deng, X. W. (2007) Analysis of transcription factor HY5 genomic binding sites revealed its hierarchical role in light regulation of development. *Plant Cell.* **19,** 731–749
58. Ramon, M., Rolland, F., and Sheen, J. (2008) Sugar sensing and signaling. *The Arabidopsis Book.* **6,** 1–22
59. Toroser, D., and Huber, S. C. (1997) Protein phosphorylation as a mechanism for osmotic-stress activation of sucrose-phosphate synthase in spinach leaves. *Plant Physiol.* **114,** 947–955